EGU General Assembly 2017
23rd – 28th April 2017
Vienna Austria

This presentation participates in OSPP
EGU Outstanding Student Poster & PICO Contest

PingPing Huang[1], Patrick Wu[1] and Wouter van der Wal[2]
[1]The University of Hong Kong, Department of Earth Sciences, Hong Kong
u3003328@hku.hk
[2]Delft University, Faculty of Aerospace Engineering, Delft, Netherlands

Effects of Mantle Rheology on Viscous Heating induced during Ice Sheet Cycles

Motivation

It was postulated that viscous heating induced by glacial cycles could induce short term heating in the mantle and transient volcanism. Using a simple parabolic ice sheet of Laurentia size, Hanyk et al.(2005) found that the viscous heating can be greater than the chondritic radioactive heating of 3×10^{-9} W/m³. Here we study the viscous heating in linear, non-linear and composite rheologies using a more realistic ice model ICE6G (Peltier, 2015). Also, we investigated the effect of viscous heating on the heat flux and temperature field of the Earth.

Modelling

We computed and compared the **viscous heating** ϕ , the perturbed **heat flux** $\vec{q}$ and **temperature anomaly** $\mathrm{T}(\vec{r},t)$ due to viscous heating for the linear model **M1**, non-linear model **M2** and composite model **M3**, all with uniform viscous property in the mantle, and linear model **M4** with VM5a profile.(See table below for viscous property). The results are shown in **Figures 1~6**.

	M1 (LINEAR)	M2 (NON-LINEAR)	M3 (COMPOSITE)	M4 (LINEAR)
$A^*(Pa^{-3}\cdot s^{-1}$ when $n=3)$	0	1.11E-34	1.11E-34	0
$\eta(Pa\cdot s)$	3.00E21	Non-linear	3.00E21	VM5a
n	1	3	3	1

A^*---non-linear parameter, η---linear viscosity, n---constant exponent

$(A^*=2A/\sqrt{3^{n+1}})$ (van der Wal et al., 2010)

Also, the viscous heat for **a wider range of A^* and η and two different Poisson's ratio** is computed, their maxima are listed in **Table 1 and Table 2**.

Viscous heating ϕ (viscous dissipation rate):

$$\phi=\frac{1}{\mu}\boldsymbol{\sigma_D}:\boldsymbol{\sigma_D}$$

$$\boldsymbol{\sigma_D}=\mu\dot{\boldsymbol{\varepsilon}}_{\boldsymbol{D}},\ \mu=\frac{1}{\frac{1}{2\eta}+A\sigma_E^{n-1}}$$

$\boldsymbol{\sigma_D}$--- the deviatoric stress tensor
$\dot{\boldsymbol{\varepsilon}}_{\boldsymbol{D}}$--- the viscous deviatoric strain rate tensor
σ_E--- the effective deviatoric stress tensor
μ--- a coefficient with the unit of viscosity. In μ,
when $A=0$ and $\frac{1}{2\eta}\neq0$, it is linear rheology;
when $A\neq0$ and $\frac{1}{2\eta}=0$, it is non-linear rheology;
when $A\neq0$ and $\frac{1}{2\eta}\neq0$, it is composite rheology.

The heat equation with ϕ as heat source:

$$\phi(\vec{r},\mathrm{t})=\rho C\frac{\partial T(\vec{r},t)}{\partial t}+\vec{\nabla}\cdot\vec{q}(\vec{r},t)$$

ρ---density, C---heat capacity
$\vec{r}$---radius, t---time

$$q(r,\theta,\varphi,t)=\int_{CMB}^{r}\phi(r',\theta,\varphi,t)r'^2dr'/r^2$$

$$T(r,\theta,\varphi,t)=\int_{26KBP}^{t}\phi(r',\theta,\varphi,t')dt'/\rho C$$

Conclusion

1. The distribution and magnitude of the viscous heat is decided by the ice history and the rheology, but the time when maximum viscous heat appears is controlled by the ice history only.

2. The viscous heat in M2 and M3 is more concentrated than that in M1, but does not extend as deep into the mantle as that in M1. The non-linear effect is dominant in the composite rheology of M3.

3. The viscous heat in M4 is more irregular but focused near in the upper mantle due to viscosity stratification, and its maximum is as large as 22.36 times that of the chondritic radiogenic heating.

4. The heat flux due to viscous heating can reach the order of magnitude of mW/m^2, while shear heating has an insignificant effect on temperature and cannot affect volcanism and rock properties(e.g. seismic speed, viscosity).

Reference
1. Hanyk, L., Matyska, C., & Yuen, D. A. (2005). Short time-scale heating of the Earth's mantle by ice-sheet dynamics. Earth, planets and space, 57(9), 895-902
2. Van der Wal, W., P. Wu, H. Wang & M.G. Sideris, (2010). Sea levels and uplift rate from composite rheology in glacial isostatic adjustment modeling, J. Geod., J. Geod., 50:38-48.
3. Peltier, W., Argus, D., and Drummond, R. (2015). Space geodesy constrains ice age terminal deglaciation: The global ICE-6G_C (VM5a) model. Journal of Geophysical Research: Solid Earth, 120(1): 450-487.

7

Result summary for a wider range of A^*, η and Poisson's ratio

ϕ_{MAX}		$\eta(Pa\cdot s)$			
		Non-linear	3.00E+20	3.00E+21	3.00E+22
A^* $(Pa^{-3}\cdot s^{-1})$	0.00E+00		11.64	3.95	0.54
	1.11E-36	2.23	11.64	6.14	2.73
	1.11E-35	9.99	11.45	11.45	10.24
	1.11E-34	10.14	9.58	10.04	10.12
	1.11E-33	6.53	6.73	6.55	6.54

Table 1: The maximum local viscous heat (in **3×10^{-9} W/m³**) of all time for different combinations of A^* and η

ϕ_{MAX}		$A^*=0$ $\eta=3E21$	$A^*=1.11E-34$ (non-linear)	$A^*=1.11E-34$ $\eta=3E21$
Poisson's ratio	0.4999	3.95	10.14	10.04
	0.2877	6.18	10.59	10.40

Table 2: The maximum local viscous heat(in **3×10^{-9} W/m³**)) at all time is shown for two values of Poisson's ratio (i.e. compressibility) with various rheology (A^* $(Pa^{-3}\cdot s^{-1})$ and $\eta(Pa\cdot s)$)

Results for M1~M4

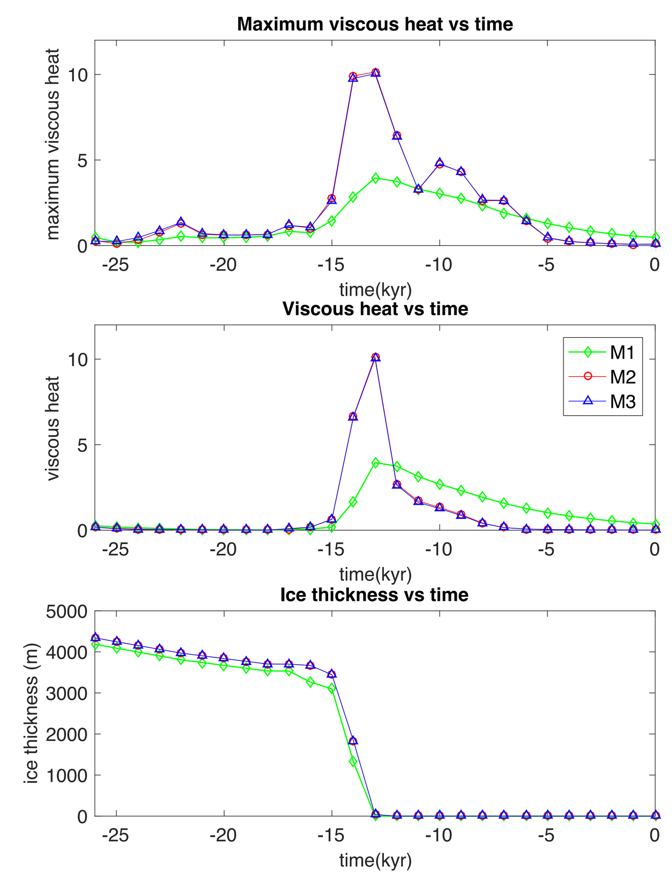

1

Figure 1: the first row shows the maximum local viscous heat in M1, M2 and M3 from 26 thousand years before present time(KBP) to the present ; the second row shows the viscous heat dependence on time for the site with the maximum viscous heat of all time; the third row gives the ice history of that site. M2 and M3 share the same site which is different from that of M1

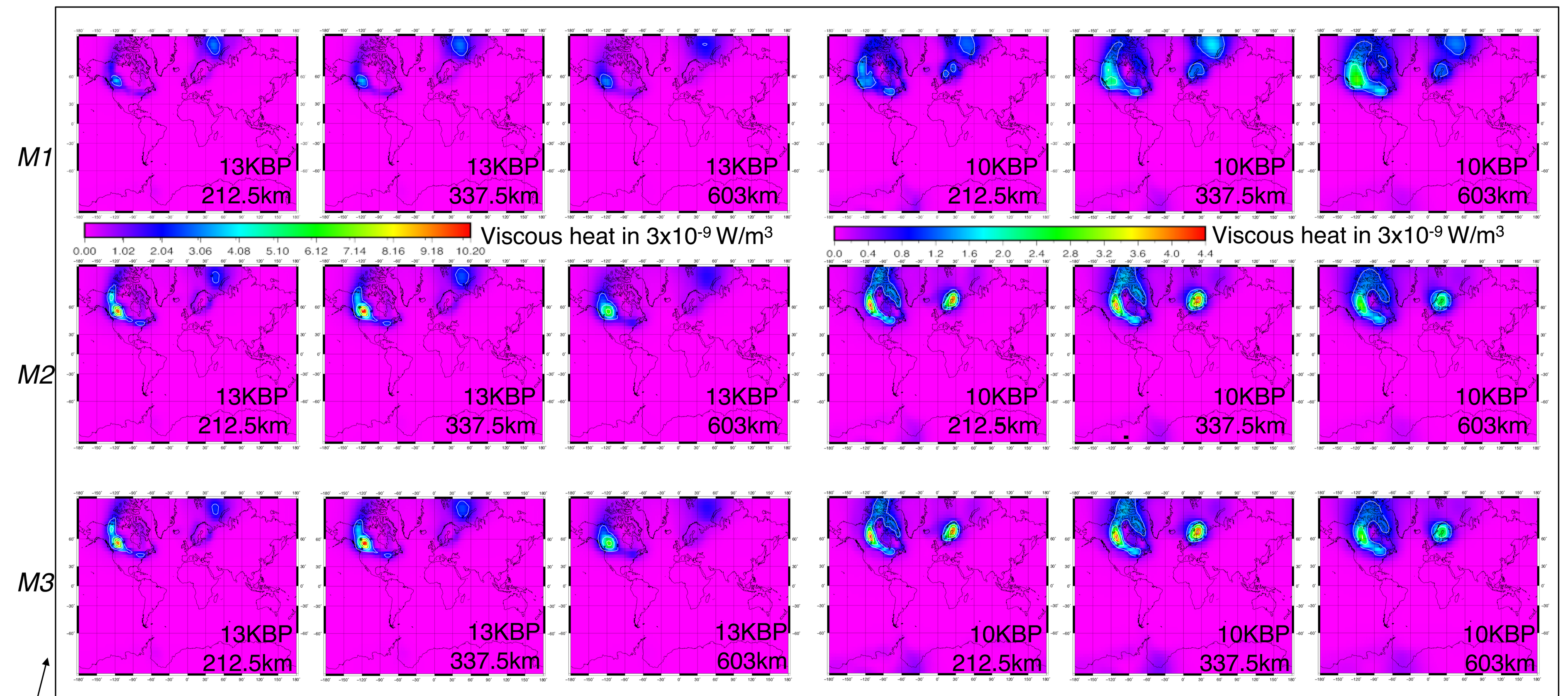

2

*Figure 2: the **viscous heat** in different depths at 13KBP (left panel) and 10KBP (right panel) for models M1, M2 and M3*

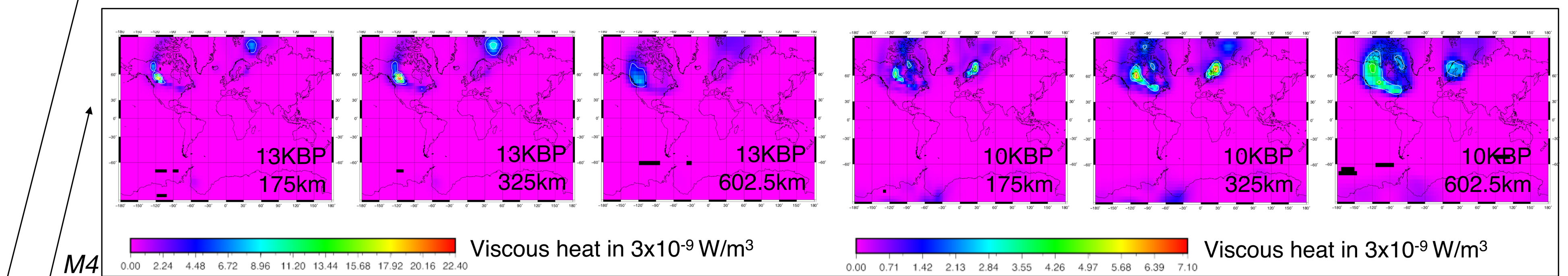

3

*Figure 3: the **viscous heat** in different depths at 13KBP(left panel) and 10KBP(right panel) for model M4*

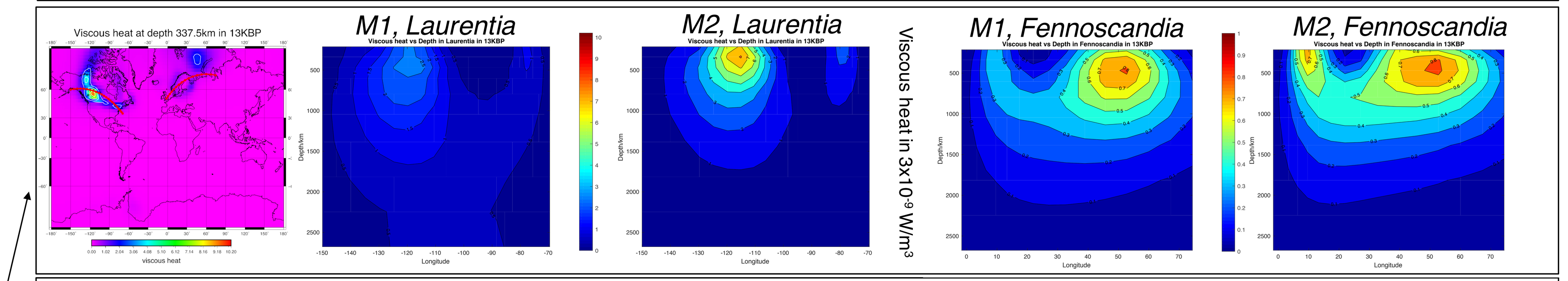

4

***Figure 4**: **cross section view of viscous heat** in Laurentia and Fennoscandia in 13KBP*

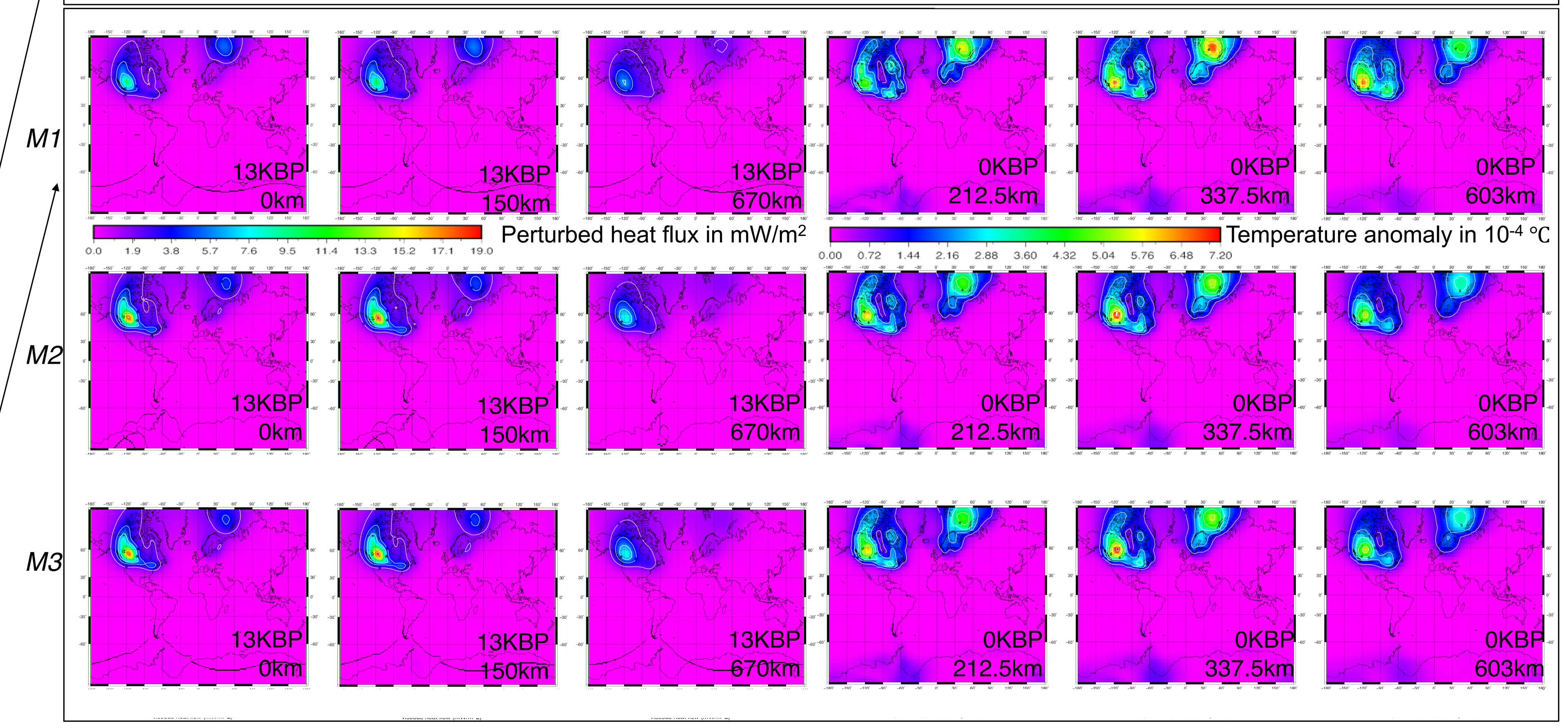

5

*Figure 5: left panel: the perturbed **heat flux** in different depths at 13KBP for models M1, M2 and M3 right panel: the **temperature anomaly** in different depths at 0KBP for models M1, M2 and M3*

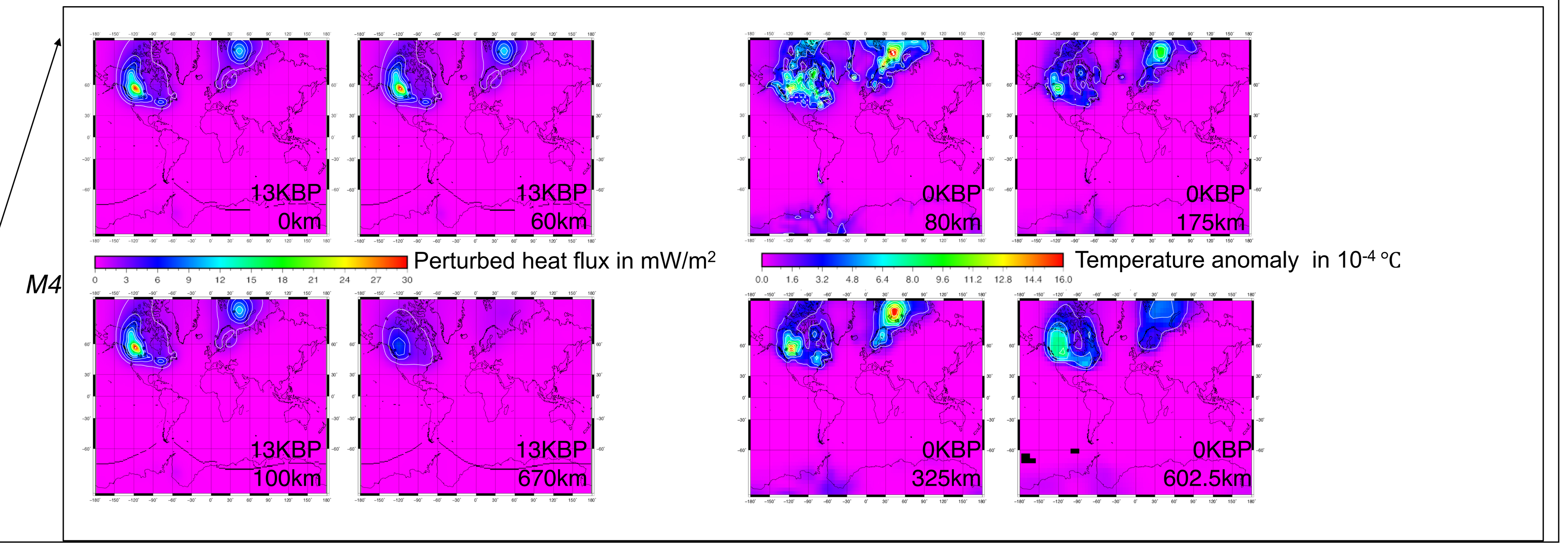

6

*Figure 6: left panel: the perturbed **heat flux** in different depths at 13KBP for model M4 right panel: the **temperature anomaly** in different depths at 0KBP for model M4*